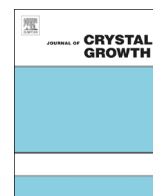




ELSEVIER

Contents lists available at ScienceDirect

Journal of Crystal Growth

journal homepage: [www.elsevier.com/locate/jcrysgro](http://www.elsevier.com/locate/jcrysgro)

# Growth and optical properties of ZnTe quantum dots on ZnMgSe by molecular beam epitaxy



W.C. Fan<sup>a</sup>, S.H. Huang<sup>a</sup>, W.C. Chou<sup>a,\*</sup>, M.H. Tsou<sup>a</sup>, C.S. Yang<sup>b</sup>, C.H. Chia<sup>c</sup>,  
Nguyen Dang Phu<sup>d</sup>, Luc Huy Hoang<sup>d</sup>

<sup>a</sup> Department of Electrophysics, National Chiao Tung University, HsinChu 30010, Taiwan, ROC

<sup>b</sup> Graduate Institute of Electro-Optical Engineering, Tatung University, Taipei 104, Taiwan, ROC.

<sup>c</sup> Department of Applied Physics, National University of Kaohsiung, Kaohsiung 81148, Taiwan, ROC

<sup>d</sup> Department of Physics, Hanoi National University of Education, 136 Xuanthuy Cauaiy, Hanoi, Vietnam

## ARTICLE INFO

Available online 7 May 2015

Keywords:

A3. Molecular beam epitaxy

B1. Nanomaterials

B1. Zinc compounds

B2. Semiconducting II–VI materials

## ABSTRACT

Self-assembled type-II ZnTe quantum dots (QDs) were grown on GaAs (001) substrates with Zn<sub>1-x</sub>Mg<sub>x</sub>Se ( $x=0.24$  and  $0.52$ ) buffer layers by molecular beam epitaxy. The optical properties of ZnTe QDs were investigated by low-temperature photoluminescence (PL) and time-resolved PL. An abrupt variation of the PL peak energy with coverage implies the existence of wetting layer of 3.2 MLs and 4.0 MLs for the Mg concentration  $x=0.24$  and  $0.52$ , respectively. The thickness of wetting layer is larger than that of ZnTe QDs grown on ZnSe buffer layers because the strain between ZnTe and Zn<sub>1-x</sub>Mg<sub>x</sub>Se is smaller. The non-mono-exponential decay profiles reflect the processes of carrier transfer and recapture. The Kohlrausch's stretching exponential well fits the decay profiles of ZnTe/Zn<sub>1-x</sub>Mg<sub>x</sub>Se QDs.

© 2015 Elsevier B.V. All rights reserved.

## 1. Introduction

Compared with quantum dots (QDs) of type-I band alignment, type-II QDs exhibit unique physical properties. The interesting physical property of optical Aharonov–Bohm effect was observed in type-II ZnTe/ZnSe QDs [1,2]. Type II InAs/GaAs/GaAs<sub>0.82</sub>As<sub>0.18</sub> QDs of long lifetime could be used for the application of high efficiency absorber in solar cell [3]. The formation of robust magnetic polaron was investigated in the ZnMnTe/ZnSe QDs [4]. However, the self-assembled QDs inevitably encounter the problem of size non-uniformity for the potential device application. The thickness of the wetting layer of the ZnMnTe/ZnSe QDs grown by the Stranski–Krastanov growth mode is fixed at 2.4 monolayers (MLs). In order to control the wetting layer thickness, dot size, dot density and the dot size uniformity, ZnTe QD structures were grown on Zn<sub>1-x</sub>Mg<sub>x</sub>Se by molecular beam epitaxy (MBE). When parts of Zn atoms of ZnSe were replaced by Mg atoms to crystallize as Zn<sub>1-x</sub>Mg<sub>x</sub>Se, the lattice constant increases because of Mg having larger ionic radius than that of Zn atom. Therefore, the manipulation of Mg concentration ( $x$ ) offers an extra degree of freedom to control the lattice mismatch between ZnTe and

Zn<sub>1-x</sub>Mg<sub>x</sub>Se and to adjust the wetting layer thickness, dot size and dot density.

## 2. Experimental methods

The samples studied in this paper were grown on GaAs (100) substrates by MBE system. Prior to the growth procedure, GaAs (100) substrates were etched in the NH<sub>4</sub>OH:H<sub>2</sub>O<sub>2</sub>:H<sub>2</sub>O (5:1:50) solution for two minutes at room temperature, rinsed in flowing de-ionized water about two minutes and dried with high purity N<sub>2</sub>. Desorption and growth procedures were monitored by the reflection high energy electron diffraction (RHEED). The growth processes of ZnTe QDs started with the deposition of Zn<sub>1-x</sub>Mg<sub>x</sub>Se buffer layer, and the alternating supply method of ZnTe growth. The coverage of the single ZnTe QDs layer, grown on the flat Zn<sub>1-x</sub>Mg<sub>x</sub>Se buffer layer, was varied from 2.4 to 4.4 MLs for Zn<sub>1-x</sub>Mg<sub>x</sub>Se buffer layer of  $x=24\%$  and 3.0 to 6.0 MLs for  $x=52\%$ . Finally, Zn<sub>1-x</sub>Mg<sub>x</sub>Se capping layer was grown on the QDs for optical measurements. Samples were also grown without Zn<sub>1-x</sub>Mg<sub>x</sub>Se capping layer for the morphology study using atomic force microscopy (AFM). The growth conditions of the ZnTe QDs on Zn<sub>1-x</sub>Mg<sub>x</sub>Se were listed in Table 1. The ZnTe/Zn<sub>1-x</sub>Mg<sub>x</sub>Se QDs with Mg concentration 24% and 52% are noted as series A and series B, respectively. The cell temperatures of Zn, Te and Se were set to 270 °C, 330 °C and 180 °C, respectively. The cell temperatures of Mg were 325 °C ( $x=24\%$ ) and 360 °C ( $x=52\%$ ).

\* Corresponding author. Tel.: +886 3 571 2121; fax: +886 3 572 5230.

E-mail address: [wuchingchou@mail.nctu.edu.tw](mailto:wuchingchou@mail.nctu.edu.tw) (W.C. Chou).

The substrate surface temperature was maintained at 320 °C throughout the growth of the QDs. The Mg concentration was determined by energy dispersive X-ray diffraction using a Zn<sub>1-x</sub>Mg<sub>x</sub>Se epilayer grown under the same conditions as the QDs structures.

The excitation source for conventional PL spectroscopy was a 325 nm-line of an He–Cd laser and the emissions were analyzed using a Horiba-Jobin Yvon iHR550 (1800 grooves/mm grating) spectrometer with a liquid nitrogen cooled CCD detector. For the excitation of time-resolved PL, the GaN 377 nm pulsed laser diode was used. The peak power of the pulse was estimated to be below 0.1 mW. The time-resolved PL spectra were analyzed using a high-speed photomultiplier tube. The overall time resolution of the detection system was about 300 ps.

### 3. Results and discussion

Fig. 1 shows the RHEED patterns (left) and AFM images (right) taken for the ZnTe QDs grown on ZnSe when the ZnTe coverages are 0, 1.8, 2.5, and 2.8 MLs. A clear transformation of the RHEED pattern from streaky to spotty, indicative of the onset of Stranski–Krastanow (SK) growth mode, could be observed when the coverage is above the critical thickness. The results from the RHEED patterns are further supported by the AFM images, clear QD formation starts when the effective thickness (coverage) of ZnTe is above 2.5 MLs. For the case of ZnTe QDs grown on Zn<sub>1-x</sub>Mg<sub>x</sub>Se, the RHEED patterns and AFM images are similar except that the critical thickness increases with increasing Mg concentration *x*.

**Table 1**  
Coverage of the ZnTe QDs in different Zn<sub>1-x</sub>Mg<sub>x</sub>Se matrices.

Zn <sub>1-x</sub> Mg <sub>x</sub> Se/ZnTe/Zn <sub>1-x</sub> Mg <sub>x</sub> Se			
<i>x</i> =0.24	Coverage	<i>x</i> =0.52	Coverage
A1	2.4 MLs	B1	3.0 MLs
A2	2.8 MLs	B2	3.5 MLs
A3	3.2 MLs	B3	4.0 MLs
A4	3.6 MLs	B4	4.5 MLs
A5	4.0 MLs	B5	5.0 MLs
A6	4.4 MLs	B6	6.0 MLs

Similar result was also observed for the CdTe QDs grown on Zn<sub>1-x</sub>Mg<sub>x</sub>Te by F. Tinjod et al. [5].

Fig. 2 shows the low-temperature PL spectra of series A, ZnTe QDs on Zn<sub>0.76</sub>Mg<sub>0.24</sub>Se with different ZnTe coverage thickness from 2.4 to 4.4 monolayers. The PL band between the spectral ranges of 2.9–3.1 eV is the near band edge emission (NBE) of Zn<sub>1-x</sub>Mg<sub>x</sub>Se layers. The low-energy emission band (2.0–2.5 eV)

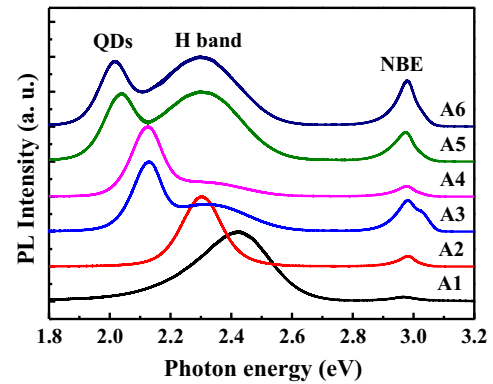


**Fig. 2.** PL spectra of ZnTe QDs on Zn<sub>0.76</sub>Mg<sub>0.24</sub>Se with different ZnTe coverages.

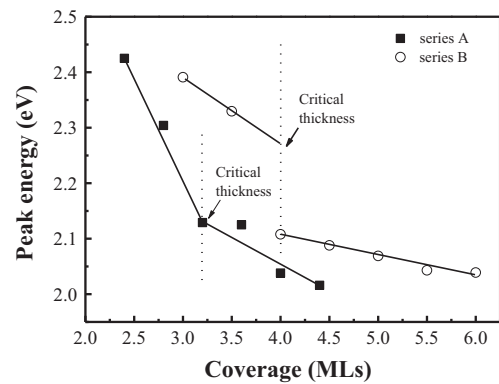


**Fig. 3.** PL emission peak energy of QD as a function of ZnTe coverage. Solid squares for ZnTe QDs self-assembled on Zn<sub>0.76</sub>Mg<sub>0.24</sub>Se; open circles for ZnTe QDs self-assembled on Zn<sub>0.46</sub>Mg<sub>0.52</sub>Se.

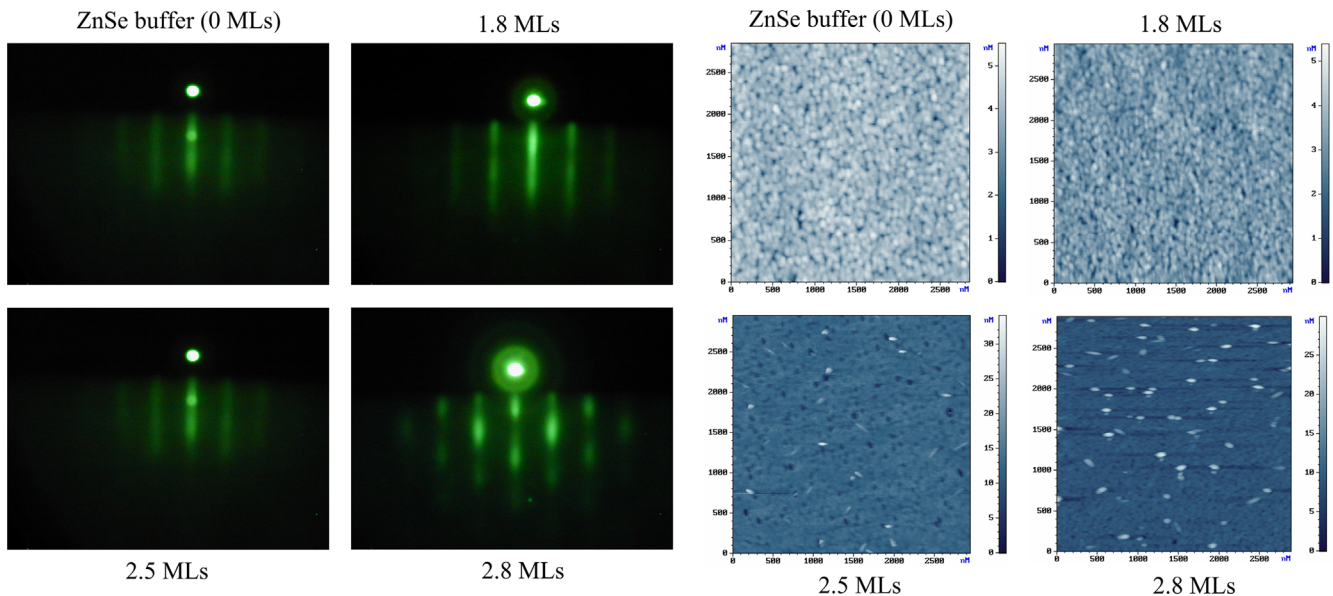


**Fig. 1.** RHEED patterns (left) and AFM images (right) taken when the ZnTe coverages are 0, 1.8, 2.5, and 2.8 MLs.

is due to the radiative recombination from QDs, because the corresponding PL peak energy is more sensitive to the change of coverage, as compared with the high-energy emission band noted as H in Fig. 2. The H emission remains constant after the dot-formation, but slightly redshifts when QDs start to form. This phenomenon is similar to the case of the two-dimensional platelet observed in the ZnMnTe QDs self-assembled on ZnSe by our previous study [6] and in CdTe QDs on ZnTe by Mackowski

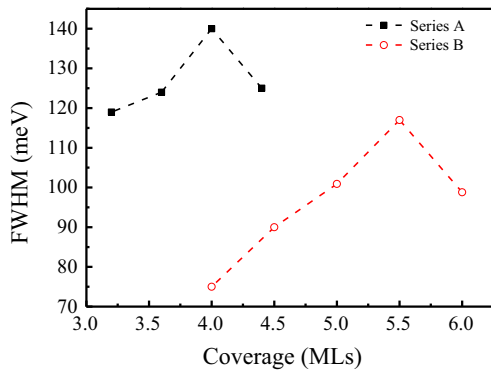


Fig. 4. FWHM change in the QDs by different coverages of ZnTe.

et al. [7]. The red-shift in QDs emission is attributed to the decrease in the quantum confinement of holes in ZnTe.

There exists a critical coverage at 3.2 MLs, judging from the two different red-shift slopes for the QD emission energy versus the ZnTe coverage for ZnTe QDs self-assembled on  $\text{Zn}_{0.76}\text{Mg}_{0.24}\text{Se}$ , as shown by the solid squares in Fig. 3. The emission energy initially red-shifts with the coverage abruptly and followed by a gentle red-shift. This is a signature of the change from the two dimensional (2-D) layer growth to 0-D QD formation for type II ZnTe QDs self-assembled on ZnMgSe in current study and also ZnMnTe QDs self-assembled on ZnSe in our previous report [6]. On the other hand, for type I CdSe QDs self-assembled on ZnSe, because both electron and hole are confined in CdSe QD, the emission energy initially red-shifts slowly and then becomes more pronounced when the coverage is above 2.5 MLs [8]. The variation of emission energy with ZnTe coverage for ZnTe QDs self-assembled on high Mg concentration  $\text{Zn}_{0.48}\text{Mg}_{0.52}\text{Se}$  is shown by the open circles in Fig. 3. The critical coverage for the change of red-shift slope is about 4.0 MLs, which is slightly larger than that of ZnTe QDs self-assembled on  $\text{Zn}_{0.76}\text{Mg}_{0.24}\text{Se}$ . It is due to the smaller lattice mismatch between ZnTe and  $\text{Zn}_{0.48}\text{Mg}_{0.52}\text{Se}$  than that between ZnTe and  $\text{Zn}_{0.76}\text{Mg}_{0.24}\text{Se}$ . This result illustrates that the thickness of the 2D wetting layer between ZnTe and  $\text{Zn}_{1-x}\text{Mg}_x\text{Se}$  can be manipulated by the control of Mg concentration  $x$ .

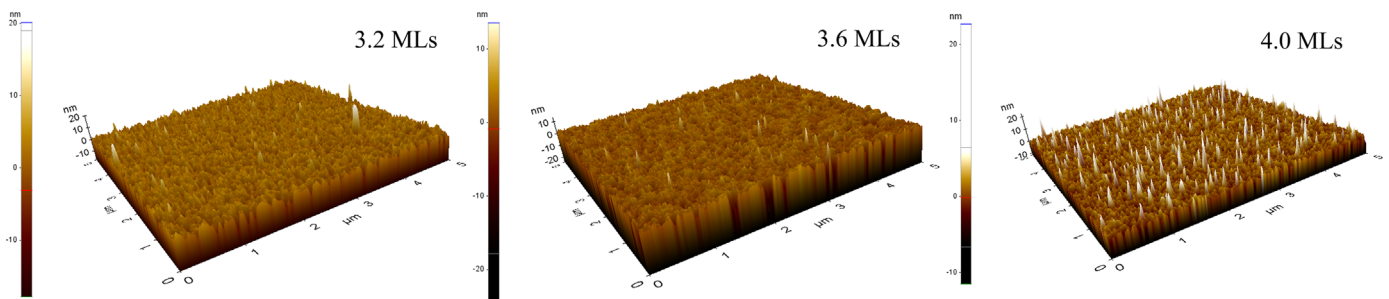


Fig. 5. AFM images of ZnTe QDs on  $\text{Zn}_{0.76}\text{Mg}_{0.24}\text{Se}$ .

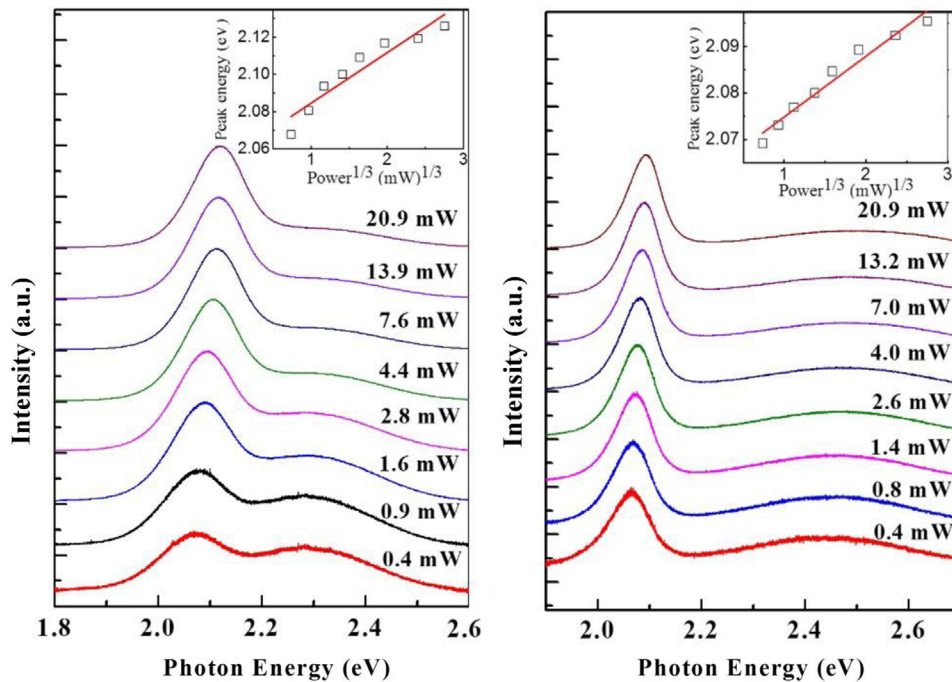


Fig. 6. PL spectra at various excitation powers: (a) for the sample A4 and (b) for the sample B4.

In Fig. 4, the full width at half maximum (FWHM) from the PL spectra of the ZnTe QDs on  $\text{Zn}_{0.76}\text{Mg}_{0.24}\text{Se}$  and ZnTe QDs on  $\text{Zn}_{0.48}\text{Mg}_{0.52}\text{Se}$  versus the ZnTe coverage are shown by the solid squares and open circles, respectively. This figure shows that all the values of FWHM in series B are smaller than that of series A. It implies that the dots size distribution in series B is more uniform than in series A. The result is similar to GeSi/Si QDs [9], which shows that the uniformity of dots improves with the decreasing mismatch between the buffer layer and QDs.

In order to study the morphology, size distribution, and dot density, the AFM images of 3.2 MLs, 3.6 MLs, and 4.0 MLs QDs on  $\text{Zn}_{0.76}\text{Mg}_{0.24}\text{Se}$  are shown in Fig. 5. The average height ( $H$ ) and diameter ( $D$ ) are 6 nm, 7 nm, 8 nm and 50 nm, 57 nm, 80 nm for the 3.2 MLs, 3.6 MLs, and 4.0 MLs samples, respectively. It confirms that dots self-assemble when the coverage of ZnTe over 3.2 MLs and also corroborates with the result obtained from two different red-shift slopes in Fig. 3. Both the size and density of QDs increases with increasing coverage of ZnTe. The densities of QDs in the samples are about the order of  $10^8/\text{cm}^2$ . In addition the non-uniformity, variation in height, increases with the ZnTe coverage. This also reflects the increasing FWHM of PL with ZnTe coverage from Fig. 4. Because, the PL emission energy is dominantly determined by the quantum confinement in height, which is much smaller than the diameter, the non-uniformity in height results the broadening in PL spectra.

In order to confirm the type-II emission nature of the ZnTe QDs on  $\text{Zn}_{1-x}\text{Mg}_x\text{Se}$ , the PL spectra under various excitation powers are shown in Fig. 6(a) and (b) for the samples A4 and B5, respectively. The PL bands blue-shift as excitation power increases. The emission peak energy linearly depends on the cubic root of the excitation power, as shown in the insets of Fig. 6. This phenomenon is caused by the band-bending effect at the hetero-interfaces [10] and is a fingerprint of the type II quantum structures. As the excitation density was increased, an increase in population of spatially confined electron-hole pairs enhanced the band-bending effect at the hetero-interfaces. In Fig. 6, there is no obvious PL band broadening with the increasing excitation power. It implies that the blue-shift of PL emission peak due to band filling effect can be excluded.

The transitions in type-II quantum structures show longer radiative lifetime than those of type-I quantum structures because of smaller overlap of electron-hole wave-functions [11]. The time-resolved PL (TRPL) measurements were carried out to study the carrier recombination dynamics in the type-II ZnTe/ $\text{Zn}_{1-x}\text{Mg}_x\text{Se}$  QDs. The temporal dependence of decay characteristics, detected at their PL peak energies, for ZnTe/ $\text{Zn}_{0.76}\text{Mg}_{0.24}\text{Se}$  QDs of different ZnTe coverages is shown in Fig. 7. The decay profiles revealed non-single-exponential decays and could be better fitted by two components. The fast component was a mono-exponential decay, while the

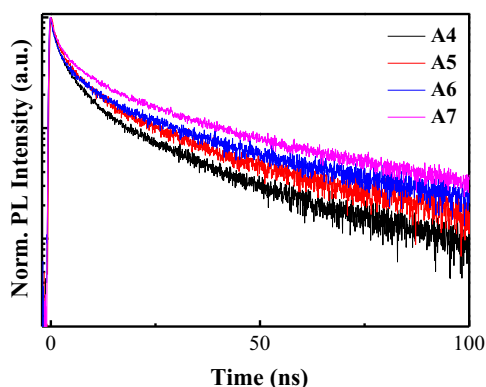


Fig. 7. The decay profiles of the PL signal, detected at their PL peak energies, from ZnTe QDs on  $\text{Zn}_{0.76}\text{Mg}_{0.24}\text{Se}$  with different ZnTe coverages.

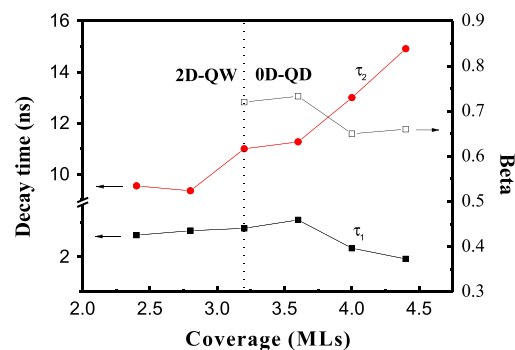


Fig. 8. Coverage dependences of decay times and  $\beta$  values obtained from the decay profiles of Fig. 6 using the profile fitting of Eq. (1).

slow component was a stretched-exponential decay. The decay curves were fitted using the following equation:

$$I_{PL}(t) = I_1 \exp(-t/\tau_1) + I_2 \exp(- (t/\tau_2)^\beta), \quad (1)$$

where  $I_{PL}(t)$  is the PL intensity at time  $t$ ,  $I_1$  and  $I_2$  are the relative intensity for fast component and slow component.  $\tau_1$  and  $\tau_2$  are lifetimes of the two different recombination mechanisms.  $\beta$  is the stretching parameter ( $0 < \beta \leq 1$ ). The best fit yields that the decay time  $\tau_1$  is about 2–3 ns for all samples and the decay time  $\tau_2$  increases with the ZnTe coverage from 10 to 15 ns.  $\tau_1$  describes the transient dynamics for carriers relaxing to QDs after the excitation. The longer time  $\tau_2$  is due to the recombination of spatially separated electron and hole after the electrons and holes are in equilibrium.

Fig. 8 shows the coverage dependences of decay times ( $\tau_1$ ,  $\tau_2$ ) and  $\beta$  values. The value of  $\beta$  always decreases and  $\tau_2$  increases with increasing thickness of ZnTe. The increase in ZnTe coverage results in the enlarged size of QDs. The larger dot size further separates the electron and hole and reduces the wave-function overlapping, which increases recombination decay time. In addition, the increase in ZnTe coverage also increases QD density. The more QDs of different sizes offer more recombination channels. For the shallow (smaller) QDs, holes could be thermally activated and transfer to the neighboring larger QDs of lower energy. As a result, the decay profiles could not be simulated by the simple single exponential  $\beta=1$ . The increasing ZnTe coverage and dot density caused the decreasing of stretching exponent  $\beta$  [12]. We also monitored the decay profiles at the emission energy of the 2-D wetting layers. The TRPL-results show that the decay time of the wetting layer is shorter than the decay time of the QDs.

#### 4. Conclusion

Self-assembled type-II ZnTe QDs were grown on GaAs (0 0 1) substrates with  $\text{Zn}_{1-x}\text{Mg}_x\text{Se}$  ( $x=0.24$  and  $0.52$ ) buffer layers by molecular beam epitaxy. Current study achieves the control of the critical thickness of Stranski–Kastanov ZnTe/ $\text{Zn}_{1-x}\text{Mg}_x\text{Se}$  QDs from 3.2 to 4.0 MLs by manipulate the Mg concentration from  $x=0.24$  to  $0.52$ . The PL decay profiles were well correlated by the Kohlrausch's stretched exponential to demonstrate the hole activation from smaller QDs followed by the transfer and re-capture to larger QDs.

#### Acknowledgments

This work was supported by the Ministry of science and technology under the grant number of MOST 103-2119-M-009-002.

## References

- [1] I.R. Sellers, V.R. Whiteside, I.L. Kuskovsky, A.O. Govorov, B.D. McCombe, *Phys. Rev. Lett.* 100 (2008) 136405.
- [2] I.R. Sellers, V.R. Whiteside, A.O. Govorov, W.C. Fan, W.C. Chou, I. Khan, A. Petrou, B.D. McCombe, *Phys. Rev. B* 77 (2008) 241302.
- [3] K. Nishikawa, Y. Takeda, T. Motohiro, D. Sato, J. Ota, N. Miyashita, Y. Okada, *Appl. Phys. Lett.* 100 (2012) 113105.
- [4] I.R. Sellers, R. Oszwaldowski, V.R. Whiteside, M. Eginligil, A. Petrou, I. Zutic, W.C. Chou, W.C. Fan, A.G. Petukhov, S.J. Kim, A.N. Cartwright, B.D. McCombe, *Phys. Rev. B* 82 (2010) 195320.
- [5] F. Tinjod, S. Moehl, K. Kheng, B. Gilles, H. Mariette, *J. Appl. Phys.* 95 (2004) 102.
- [6] M.C. Kuo, J.S. Hsu, J.L. Shen, K.C. Chiu, W.C. Fan, Y.C. Lin, C.H. Chia, W.C. Chou, M. Yasar, R. Mallory, A. Petrou, H. Luo, *Appl. Phys. Lett.* 89 (2006) 263111.
- [7] S. Mackowski, G. Prechtel, W. Heiss, F.V. Kyrychneko, G. Karczewski, J. Kossut, *Phys. Rev. B* 69 (2004) 205325.
- [8] Y.J. Lai, Y.C. Lin, C.B. Fu, C.S. Yang, C.H. Chia, D.S. Chuu, W.K. Chen, M.C. Lee, W.C. Chou, M.C. Kuo, J.S. Wang, *J. Cryst. Growth* 282 (2006) 338.
- [9] G. Abstreiter, P. Schittenhelm, C. Engel, E. Silveira, A. Zrenner, D. Meertens, W. Jager, *Semiconduct. Sci. Technol.* 11 (1996) 1521.
- [10] N.N. Ledentsov, J. Böhrer, M. Beer, F. Heinrichsdorff, M. Grudmann, D. Bimberg, S.V. Ivanov, B. Ya., S.V. Meltser, I.N. Shaposhnikov, N.N. Yassievich, P.S. Faleev, Kop'ev, Z.h.I. Alferov, *Phys. Rev. B* 52 (1995) 14058.
- [11] Jai Verma, S.M. Islam, Vladimir Protasenko, Prem Kumar Kandaswamy, Huili Xing, Debdeep Jena, *Appl. Phys. Lett.* 104 (2014) 021105.
- [12] B. Sturman, E. Podivilov, M. Gorkunov, *Phys. Rev. Lett.* 91 (2003) 176602.